Eidgenössische Technische Hochschule Zürich
Swiss Federal Institute of Technology Zurich

Seminar for Applied Mathematics SAM

Hybridization of Singular Plasmons via Transformation Optics

S. Yu and H. Ammari

Research Report No. 2018-26

July 2018
Latest revision: July 2018

Seminar für Angewandte Mathematik
Eidgenössische Technische Hochschule
CH-8092 Zürich
Switzerland

Hybridization of Singular Plasmons via Transformation Optics

Sanghyeon Yu*† Habib Ammari*

Abstract

Strongly interacting metallic nanoparticles are useful for controlling light at the nanoscale due to their surface plasmons. Here we develop a new physical model for understanding plasmons of interacting particles. We combine both the hybridization model and transformation optics so that our model gives a simple and intuitive picture when the particles are close-to-touching. In the proposed approach, the system's plasmon is a combination of the gap-plasmons of each pair of particles. This provides new physical insights into how the spectrum of the plasmons depends on global and local features of the geometry.

1 Manuscript

Metallic nanostructures have been extensively studied and utilized for sub-wavelength control of light due to their unique ability to support surface plasmons, which are oscillations of electron density on metal-dielectric interfaces [1–6]. Among various structures, a system of interacting nanoparticles is of fundamental importance [6]. When the particles are closely spaced, their plasmons exhibit significant spectral shifts, extreme light confinement, and Fano resonances [5] due to their strong electromagnetic interaction. These phenomena have important applications including optical nanocircuits, single molecule sensing, spectroscopy, and nonlinear optics [1–6]. But understanding the strong interaction between the particles is quite challenging because plasmons depend on the geometry of the particles in a complicated way. It is important to clarify their deep relation for a rational design of plasmonic devices.

The plasmon hybridization model results in a simple and intuitive physical picture for plasmons of interacting particles in a way analogous to molecular orbital theory, providing a general and powerful design principle [6–8]. In this model, the hybridized plasmons are viewed as simple combinations of the individual particle plasmons. However, when the particles become close-to-touching, the picture becomes complicated since a large number of uncoupled plasmons contribute to each hybridized plasmon. Recently, Transformation Optics (TO) has been applied to two close-to-touching particles and other singular plasmonic structures [9–11]. We also refer to [12–22] for related works. TO has revealed that, as the particles get closer, light is strongly confiend to the narrow gap for a broad band of frequencies. TO also provides an exact analytic description. But TO alone cannot be applied to systems featuring three (or more) particles.

In this work, we develop a new hybridization model for plasmons of strongly interacting many-particle systems. Our model combines the advantages of both the hybridization and

*Department of Mathematics, ETH Zürich, Rämistrasse 101, CH-8092 Zürich, Switzerland.
†Correspondence to S.Y. (sanghyeon.yu@sam.math.ethz.ch)

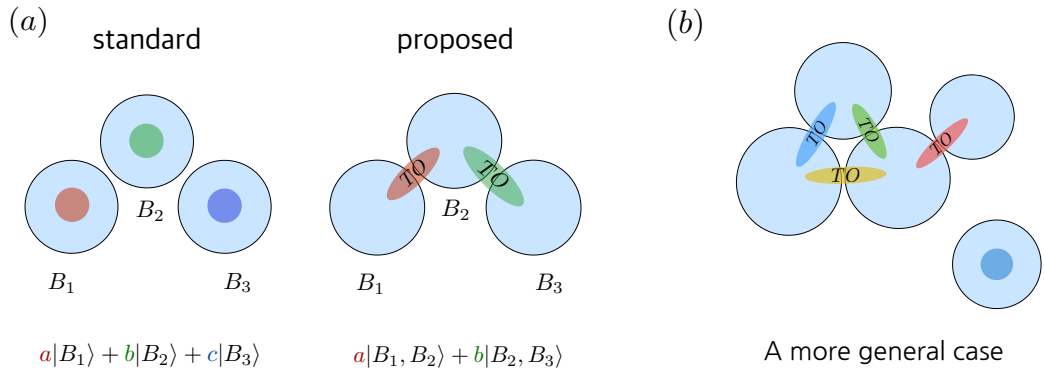

Figure 1: Schematic description of our proposed model. (a) comparison with the standard hybridization model. (b) a more general system of interacting particles.

TO approaches, thus providing a simple and intuitive picture when the particles are close-to-touching. More importantly, the proposed model leads to new physical insights into the relation between geometry and plasmons: how global and local features of the system's complex geometry affect the spectrum of the plasmons. Our model enables us to decompose the spectrum into singularly and regularly shifted parts. The singular (resp. regular) part is controlled by local (resp. global) features of the geometry. Our model informs us how we can control them in a systematic way, opening up new degrees of freedom for light manipulation at the nanoscale.

Before explaining our model, we mention that the non-local effect, which has a quantum origin, is an important issue when the gap distance is extremely small (below 0.5nm) [23–28]. Our focus is *not* on modelling the non-local effect but on understanding the strong interaction between the particles. We shall assume the local model for the metal permittivity. The nonlocal effect can be accounted for by using the approach of [10, 25, 26].

We now explain our proposed model which we call the *Singular Hybridization (SH) Model*. In the standard hybridization model, a plasmon of the system is a combination of plasmons of individual particles. On the contrary, in our approach, the basic building blocks are the gap-plasmons of a pair of particles, and for these we use the TO approach. This simple conceptual change is the key to solving the aforementioned challenges. Let us consider a trimer, shown in Figure 1a, as it is the simplest example for our model (we emphasize that our model can be applied to a general configuration of particles as shown in Figure 1b). The trimer plasmon is now treated as a combination of two gap-plasmons. For each gap-plasmon, we use TO to capture the singular spectral shift. In our picture, the new plasmons are formed by the hybridization of singular gap-plasmons. The gap-plasmons are strongly confined in their respective gaps and all the gaps are well-separated, which means that the gap-plasmons do not overlap significantly with each other. Hence, the spectral shifts due to their hybridization should be moderate. Therefore, we can expect that we still get a simple picture even in the close-to-touching case.

To gain a better understanding, we develop a coupled mode theory for the hybridization of singular plasmons. For simplicity, we only consider 2D structures, however, our theory can be extended to the 3D case. We assume the Drude model for the metal permittivity: $\varepsilon = 1 - \frac{\omega_p^2}{\omega^2}$,

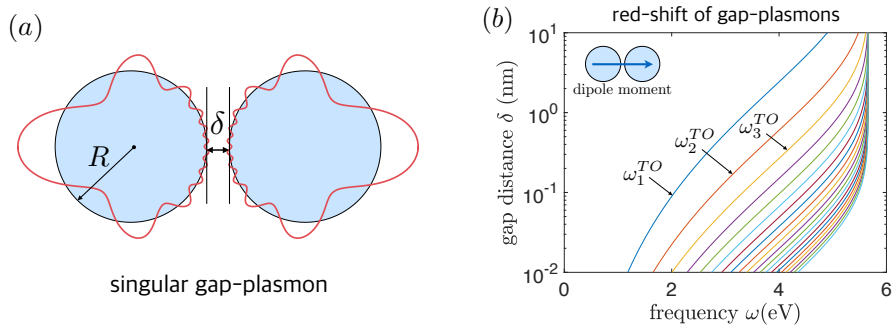

Figure 2: Singular gap-plasmons of the dimer. (a) the dimer and its gap-plasmon. (b) The red-shift of the resonance frequencies ω_n^{TO} as a function of the gap distance. We set $R = 20$nm and $\omega_p = 8$eV.

where ω_p is the bulk plasma frequency and the background permittivity is $\varepsilon_0 = 1$. We also adopt the quasi-static approximation by assuming the particles system to be small compared to the wavelength of the incident light. We remark that the radiation reaction can be incorparated as described in [10].

We briefly review the TO description [29] of gap-plasmons which are the basic building blocks of our proposed model. Consider a dimer of cylinders of radii R separated by a distance δ. TO provides both physical pictures and analytic solutions for the dimer gap-plasmons. When the two cylinders get closer, the wavelength of their plasmon near the gap get smaller and energy accumulates there giving rise to the extreme field enhancement (Figure 2a). The spectrum also exhibit a singular behavior. Let us consider only the plasmons whose dipole moment is aligned parallel to the dimer axis since these plasmons contribute to the optical response significantly. The resonance frequencies ω_n^{TO} of the dimer gap-plasmons are given by

$$\omega_n^{TO} = \omega_p \sqrt{e^{-ns} \sinh(ns)}, \quad n = 1, 2, 3, \cdots,$$

with the parameter s satisfying $\sinh^2 s = (\delta/R)(1 + \delta/4R)$. We denote their associated gap-plasmon modes by $|\omega_n^{TO}\rangle$. When the gap distance δ gets smaller, as shown in Figure 3c, the frequencies ω_n^{TO} are red-shifted singularly and the spectrum becomes more dense, which allows for broadband light-harvesting to a singular point (the gap center). In the touching limit, the spectrum becomes continuous if we neglect the nonlocal effect. Thus, the TO description captures the singular behavior of gap-plasmons $|\omega_n^{TO}\rangle$.

We now turn to our model. We explain our model taking a trimer as an example (Figure 3a). The plasmons of the trimer are specified as a superposition of the gap-plasmon of the pair (B_1, B_2) and that of the pair (B_2, B_3). We let (a_n, b_n) represent the following linear combination of the gap-plasmons: $a_n|\omega_n^{TO}(B_1, B_2)\rangle + b_n|\omega_n^{TO}(B_2, B_3)\rangle$. Their hybridization is characterized by the following coupled mode equations:

$$\begin{bmatrix} (\omega_n^{TO})^2 & \Delta_n \\ \Delta_n & (\omega_n^{TO})^2 \end{bmatrix} \begin{bmatrix} a_n \\ b_n \end{bmatrix} = \omega^2 \begin{bmatrix} a_n \\ b_n \end{bmatrix}.$$

Here, Δ_n represents the coupling between the two gap-plasmons. This coupled mode system

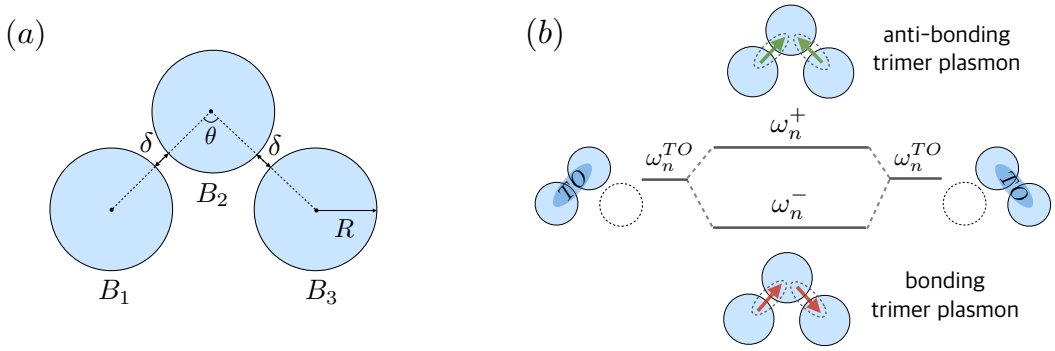

Figure 3: Trimer plasmons. (a) geometry of the trimer. (b) the hybridization picture for the trimer plasmon: the bonding and anti-bonding combinations of singular gap-plasmons.

is derived using the spectral theory of the Neumann–Poincaré operator [30–32] and TO (See Supplemantary Material for the details and the expression for Δ_n). We emphasize that the above equation is a simplified version of our theory. Although we require additional TO modes for improved accuracy, we shall see that this simplified version can already capture the physics. Solving the equation, we obtain the hybrid plasmons for the trimer:

$$|\omega_n^{\pm}\rangle \approx \frac{1}{\sqrt{2}}\Big(|\omega_n^{TO}(B_1,B_2)\rangle \mp |\omega_n^{TO}(B_2,B_3)\rangle\Big), \quad n=1,2,3,\cdots,$$

and their resonance frequencies

$$\omega_n^{\pm} \approx \omega_n^{TO} \pm \Delta_n, \quad n=1,2,3,\cdots.$$

As the bonding angle θ between the two gap-plasmons decreases, the coupling strength Δ_n increases, which is to be expected since the two gaps get closer. So our theory predicts that the spectrum consists of a family of pairs (ω_n^-, ω_n^+) of resonance frequencies which are split from the dimer resonance frequencies ω_n^{TO}. The frequency ω_n^{TO} is singularly shifted as the gap distance δ get smaller as already mentiond. But the splitting Δ_n remains moderate. We call $|\omega_n^-\rangle$ and $|\omega_n^+\rangle$ the *bonding trimer plasmon* and *anti-bonding trimer plasmon*, respectively (Figure 3b). The bonding plasmon has a net dipole moment in the x-direction so it can be excited by x-polarized light. Similarly, the anti-bonding plasmon can be excited by y-polarized light. These plasmons are very different from the bonding plasmon and anti-bonding plasmon of a dimer in the standard hybridization model. They are trimer plasmons and are capable of capturing the close-to-touching interaction via TO.

We now discuss the physical implications of our SH model. The power of our model comes from its ability to decompose the spectrum into a singular part, which depends on the local geometry, and a regular part, which depends on the global geometry. The resonance frequency $\omega_n^{\pm}$ for the trimer consists of two parts: the singularly shifted part ω_n^{TO} and the regular splitting part Δ_n. The singular part ω_n^{TO} is determined by the small gap distance δ, which is a 'local' feature of the geometry. On the other hand, the regular part Δ_n is determined by the bonding angle θ, which is a 'global' feature of the geometry. In other words, the small gap distance δ affects the

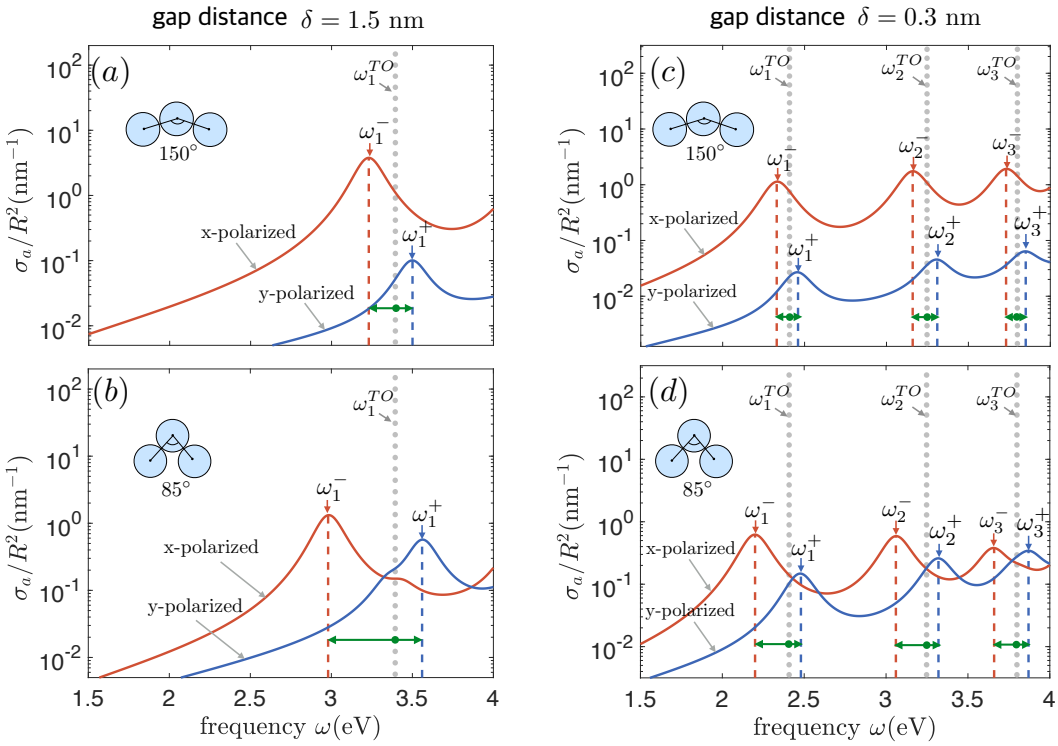

Figure 4: Absorption cross section σ_a for the trimer. (a,b) The red (or blue) solid line represents the case of the x-polarized (or y-polarized) incident field, respectively. We set the radius $R = 30$ nm and the gap distance $\delta = 1.5$ nm. (c,d) the same but with a smaller gap distance $\delta = 0.3$ nm.

'overall' behavior of the spectrum while the bonding angle θ controls the 'detailed' splitting of the spectrum. This shows an interesting relation between the spectrum and the geometry: *local* (and *global*) features of the geometry can determine the *global* (and *local*) behavior of the spectrum, respectively. This relation provides us with a design principle: manipulation of the local geometrical singularity (such as inter-particle gap distances) to control the overall behavior of the spectrum, together with manipulation of the global geometry to achieve detailed splittings of the spectrum. Our SH model provides a systematic way of achieving such a design using gap-plasmons as basic building blocks. We emphasize that our approach is valid for general systems consisting of an arbitrary number of interacting particles, with arbitrary positions and different radii.

We validate our model with numerical examples for the trimer. We set the radius of the particles to be $R = 30$ nm. We consider two cases: when the inter-particle gap distance are (i) $\delta = 1.5$ nm and (ii) $\delta = 0.3$ nm. Notice that the ratio δ/R is very small so that the particles are nearly touching. We assume the Drude model $\epsilon = 1 - \omega_p^2/(\omega(\omega + i\gamma))$ with $\omega_p = 8$ eV and $\gamma = 0.2$ eV. In Figures 3a and 3b, we plot the absorption cross section for the trimer with the gap distance $\delta = 1.5$ nm when the bonding angle is $\theta = 140°$ (weak coupling) and $\theta = 50°$ (strong coupling), respectively. In the latter case, the coupling strength between the

gap-plasmons is stronger since the gaps are closer to each other. Similarly, in Figures 3c and 3d, we plot the absorption cross section in the case of the smaller gap distance $\delta = 0.3$ nm. We also plot the values of the resonance frequencies ω_n^- and ω_n^+ (red and blue dashed lines) computed by a complete version of our theory. Their corresponding plasmons are dominated by bonding and anti-bonding combinations, respectively. As expected, the resonance peaks of the absorption are located near the bonding (and anti-bonding) plasmon frequencies ω_n^- (and ω_n^+) for the x-polarized (and y-polarized) incident field, respectively. The gray dots represent the dimer frequency ω_n^{TO} computed using the TO approach. As the gap-distance δ gets smaller, the overall spectrum is significantly red-shifted in conjunction with the singular shift of ω_n^{TO}. The green arrows represents how much the trimer frequencies $\omega_n^{\pm}$ are split from the dimer frequency ω_n^{TO}. The splittings $\omega_n^{\pm} - \omega_n^{TO}$ are also clearly shown and it is moderate regardless of the inter-particle gap-distance. In the strong coupling case (smaller bonding angle), the splittings are more pronounced. Also, the absorption of the y-polarized incident field becomes stronger since the net dipole moment of the anti-bonding mode increases as the bonding angle θ decreases. Hence, the numerical results are consistent with the prediction of our proposed SH Model.

In summary, we have proposed the *Singular Hybridization Model* for understanding singular plasmons of strongly interacting particles. The proposed model demonstrates an elegant interplay between the hybridization picture and transformation optics. It provides a new means of understanding plasmonic interactions while clarifying a deep geometrical dependence of the spectrum. We believe that our model can have a significant impact on the design of future plasmonic devices. The extension to the 3D case and incorporating the retardation effect beyond the quasi-static approximation will be considered elsewhere.

2 Supplementary Materials

Here we outline our coupled mode theory for the hybridization of singular plasmons. We consider the 2D case for simplicity. We also assume the quasi-static approximation.

Integral equation approach for surface plasmons. Suppose we have a system of nanoparticles Ω with permittivity ϵ. We assume the background permittivity $\epsilon_0 = 1$ and the incident electric field $\mathbf{E}^{in}$. Then the induced charge density σ on the surfaces $\partial\Omega$ of the particles is determined by the following integral equation [30–32]:

$$(\mathcal{K}_\Omega^* - \lambda I)[\sigma] = \mathbf{E}^{in} \cdot \mathbf{n}, \quad \lambda = \frac{\epsilon + 1}{2(\epsilon - 1)},$$

where $\mathcal{K}_\Omega^*$ is the Neumann–Poincaré (NP) operator given by

$$\mathcal{K}_\Omega^*[\sigma](\mathbf{r}) = \frac{1}{2\pi} \int_{\partial\Omega} \frac{(\mathbf{r} - \mathbf{r}') \cdot \mathbf{n}_\mathbf{r}}{|\mathbf{r} - \mathbf{r}'|^2} \sigma(\mathbf{r}') dS(\mathbf{r}'), \quad \mathbf{r} \in \partial\Omega.$$

and $\mathbf{n}$ is the outward unit normal vector to the surface. If the permittivity ϵ is negative, then the above problem admits a solution even when the incident field $\mathbf{E}^{in}$ is absent. In fact, this solution corresponds to the (localized) surface plasmon of the particle. More precisely, the mathematical analysis of the surface plasmons is equivalent to the following eigenvalue problem for the NP

operator [30–32]:

$$\mathcal{K}_\Omega^*[\sigma] = \lambda\sigma, \quad \lambda = \frac{\epsilon+1}{2(\epsilon-1)}.$$

If we model the metal permittivity by Drude's model in which $\epsilon = 1 - \frac{\omega_p^2}{\omega^2}$, then the above eigenvalue problem can be rewritten as

$$\mathcal{A}_\Omega[\sigma] := \omega_p^2\Big(\frac{1}{2}I - \mathcal{K}_\Omega^*\Big)[\sigma] = \omega^2\sigma.$$

Let ω_n^2 and σ_n be the eigenvalues and eigenfunctions of the operator $\mathcal{A}_\Omega$. Then ω_n (and σ_n) of the operator $\mathcal{A}_\Omega$ represents the resonance frequency (and the charge density) of plasmons, respectively. Let us denote the plasmon charge density σ_n by $|\omega_n\rangle$ to indicate that its resonance frequency is ω_n.

Let us define an inner product $\langle\omega_n|\omega_{n'}\rangle$ of two plasmons $|\omega_n\rangle$ and $|\omega_{n'}\rangle$ by

$$\langle\omega_n|\omega_{n'}\rangle = \int_{\partial\Omega}\sigma_n(\mathbf{r})\int_{\partial\Omega}\frac{(-1)}{2\pi}\log|\mathbf{r}-\mathbf{r}'|\sigma_{n'}(\mathbf{r}')dS(\mathbf{r}')dS(\mathbf{r}).$$

It can be shown that the eigenfunctions of the operator $\mathcal{K}_\Omega^*$ (hence $\mathcal{A}_\Omega$) form a complete orthogonal basis with respect to the above inner product.

TO description of the dimer plasmons. Consider the dimer $D = B_+ \cup B_-$ where $B_\pm$ is a circular cylinder of radius R centered at $\pm(R+\delta/2, 0)$. Note that the two particles B_+ and B_- are separated by a distance δ. Using the TO approach, we can derive the dimer plasmons (*i.e.* the eigenvalues and eigenfunctions of the operator $\mathcal{A}_D$) explicitly. The conformal transformation Φ given by

$$x' + iy' = \Phi(x+iy) = \frac{x+iy+a}{x+iy-a}, \qquad a = (\delta(R+\delta/4))^{1/2},$$

maps the dimer to a concentric annulus whose inner radius is $r_i = e^{-s}$ and outer radius is $r_e = e^s$, where $\sinh s = a/R$. Let (r', θ') be the polar coordinates of the transformed frame, namely, $z' = x' + iy' = r'e^{i\theta'}$. As mentioned in the manuscript, we consider only the dimer plasmons whose dipole moment is aligned in the x-direction. Their resonance frequencies are

$$\omega_n^{TO} = \omega_p\sqrt{e^{-ns}\sinh(ns)}, \quad n = 1, 2, 3, \cdots.$$

The charge densities $|\omega_n^{TO}\rangle$ of the associated dimer plasmons are given as follows: for $n = 1, 2, 3, \cdots$,

$$|\omega_n^{TO}\rangle(\mathbf{r}) = \pm\frac{1}{\sqrt{N_n}}\frac{\cosh s - \cos\theta'}{\alpha}\cos n\theta', \quad \mathbf{r}\in\partial B_\pm,$$

where the normalization constant N_n is chosen such that $\langle\omega_n^{TO}|\omega_n^{TO}\rangle = 1$. Note that $\mathcal{A}_D|\omega_n^{TO}\rangle = (\omega_n^{TO})^2|\omega_n^{TO}\rangle$.

Hybridization of singular plasmons: a trimer case. Next, we consider the trimer $T = B_1 \cup B_2 \cup B_3$ given in the manuscript. Recall that the pairs (B_1, B_2) and (B_2, B_3) are close-to-touching while B_1 and B_3 are well-separated. After some translation and rotation and by abuse of notation, we can define the TO dimer plasmons for the pair (B_1, B_2) and the pair (B_2, B_3)

as follows:

$$|\omega_n^{TO}(B_1, B_2)\rangle = \begin{cases} \omega_n^{TO} & \text{on } \partial B_1 \cup \partial B_2, \\ 0 & \text{on } \partial B_3, \end{cases}$$

and

$$|\omega_n^{TO}(B_2, B_3)\rangle = \begin{cases} 0 & \text{on } \partial B_1, \\ \omega_n^{TO} & \text{on } \partial B_2 \cup \partial B_3. \end{cases}$$

These two dimer plasmons hybridize to form new modes. We approximate a hybridized mode $|\omega_n\rangle$ as a linear combination $|\omega_n\rangle = a_n|\omega_n^{TO}(B_1, B_2)\rangle + b_n|\omega_n^{TO}(B_2, B_3)\rangle$. This is a good approximation when the gap distance δ is small. In fact, we can prove that the set of $|\omega_n^{TO}(B_i, B_j)\rangle$ form an 'almost' orthogonal basis. More precisely, as $\delta \to 0$,

$$\langle \omega_n^{TO}(B_1, B_2)|\omega_{n'}^{TO}(B_2, B_3)\rangle \approx 0 \quad \text{for all } n, n' = 1, 2, 3, \cdots,$$

and consequently,

$$\langle \omega_n|\omega_{n'}\rangle \approx 0 \quad \text{for } n \neq n'.$$

Using the fact that $\mathcal{A}_D|\omega_n^{TO}\rangle = (\omega_n^{TO})^2|\omega_n^{TO}\rangle$, we can easily see that

$$\begin{bmatrix} (\omega_n^{TO})^2 & \Delta_n \\ \Delta_n & (\omega_n^{TO})^2 \end{bmatrix} \begin{bmatrix} a_n \\ b_n \end{bmatrix} = \omega^2 \begin{bmatrix} a_n \\ b_n \end{bmatrix},$$

where Δ_n is given by

$$\Delta_n = \langle \omega_n^{TO}(B_1, B_2)|\mathcal{A}_T|\omega_n^{TO}(B_2, B_3)\rangle.$$

By finding the eigenvalues and eigenvectors of the matrix on the LHS, we can find good approximations for the hybrid plasmons and their resonance frequencies. The interaction term Δ_n can be computed analytically using the connection between TO and the method of image charges [21]. By including a full set of basis (the gap-plasmons with different angular momenta n and the gap-plasmons for the other pair (B_1, B_3)), we can compute accurately all the resonance frequencies and their associated plasmon modes. We remark that this model is also very efficient numerically in the nearly touching case.

Although we considered only the trimer in this work, it is straightforward to extend the above coupled mode theory to a more general system with an arbitrary number of particles. Moreover, the particles do not have to be identical and can have different material parameters from each other.

References

[1] E. Ozbay, Science 311, 189-193 (2006).

[2] S. Lal, S. Link, N. J. Halas, Nature Photonics 1, 641648 (2007)

[3] D. K. Gramotnev, S. I. Bozhevolnyi, Nature Photonics, 4, 83–91 (2010).

[4] J. A. Schuller et al., Nature Materials 9, 193 (2010).

[5] B. Luk'yanchuk et al., Nature Materials 9, 707 (2010).

[6] N. J. Halas, S. Lal, W. S. Chang, S. Link, P. Nordlander, Chemical Reviews 111, 3913–3961 (2011).

[7] E. Prodan, C. Radloff, N. J. Halas, and P. Nordlander, Science 302, 419–422 (2003).

[8] P. Nordlander, C. Oubre, E. Prodan, K. Li, and M. I. Stockman, Nano Lett. 4, 899–903 (2004).

[9] J. B. Pendry, Y. Luo, and R. Zhao, Science 348, 521–524 (2015).

[10] J. B. Pendry, A. Aubry, D. R. Smith, and S. A. Maier, Science, 337 (2012), pp. 549–552.

[11] J. B. Pendry, A. I. Fernandez-Dominguez, Y. Luo, and R. Zhao, Nature Physics, 9 (2013), pp. 518–522.

[12] R.C. McPhedran and W.T. Perrins, Applied Physics A 24, 311-318 (1981).

[13] R. C. McPhedran, L. Poladian, and G. W. Milton, Proc. R. Soc. A 415, 185–196 (1988).

[14] L. Poladian, Quart. J. Mech. Appl. Math., 41, 395–417 (1988).

[15] L. Poladian. Ph.D. thesis, University of Sydney (1990).

[16] H. Ammari, G. Ciraolo, H. Kang, H. Lee, and K. Yun, Arch. Rational Mech. Anal. 208, 275–304 (2013).

[17] L. Berlyand, A. G. Kolpakov, A. Novikov. *Introduction to the network approximation method for materials modeling* (Cambridge University Press, 2013).

[18] E. Bonnetier and F. Triki, Arch. Rational Mech. Anal. 209, 541–567 (2013).

[19] M. Lim and S. Yu, J. Math. Anal. Appl. 421 , 131–156 (2015).

[20] O. Schnitzer, Phys. Rev. B 92, 235428 (2015).

[21] S. Yu and H. Ammari, SIAM Rev. 60, 356–385 (2018).

[22] O. Schnitzer, arXiv:1807.01636 (2018).

[23] J Zuloaga, E Prodan, P Nordlander, Nano Letters 9, 887-891 (2009).

[24] C. Ciraci et al., Science 337, 1072–1074 (2012).

[25] Y. Luo et al., Phys. Rev. Lett. 111, 093901 (2013).

[26] Y. Luo, R. Zhao, and J. B. Pendry, Proc. Nat. Acad. Sci. U.S.A. 111, 18422–18427 (2014).

[27] W. Zhu et al., Nature Comms. 7, 11495 (2016).

[28] O. Schnitzer, V. Giannini, R. V. Craster, and S. A. Maier, Phys. Rev. B 93, 041409 (2016).

[29] A. Aubry, D. Y. Lei, S. A. Maier, and J. B. Pendry, Phys. Rev. Lett. 105, 233901 (2010).

[30] H. Ammari, Y. Deng, and P. Millien, Arch. Ratio. Mech. Anal. 220, 109–153 (2016).

[31] K. Ando and H. Kang, J. Math. Anal. Appl. 435, 162–178 (2016).

[32] I. D. Mayergoyz, D. R. Fredkin, and Z. Zhang, Phys. Rev. B 72, 155412 (2005).